Hole-initiated multiplication in back-illuminated GaN avalanche photodiodes

R. McClintock, J. L. Pau, K. Minder, C. Bayram, P. Kung, and M. Razeghi[a)]
Center for Quantum Devices, Department of Electrical Engineering and Computer Science, Northwestern University, Evanston, Illinois 60208

(Received 15 January 2007; accepted 6 March 2007; published online 6 April 2007)

Avalanche *p-i-n* photodiodes were fabricated on AlN templates for back illumination. Structures with different intrinsic layer thicknesses were tested. A critical electric field of 2.73 MV/cm was estimated from the variation of the breakdown voltage with thickness. From the device response under back and front illumination and the consequent selective injection of holes and electrons in the junction, ionization coefficients were obtained for GaN. The hole ionization coefficient was found to be higher than the electron ionization coefficient as predicted by theory. Excess multiplication noise factors were also calculated for back and front illumination, and indicated a higher noise contribution for electron injection. © *2007 American Institute of Physics*.
[DOI: 10.1063/1.2720712]

Ultraviolet (UV) photodetectors find uses in numerous applications in the defense, commercial, and scientific arenas. GaN avalanche photodiodes (APDs) present themselves as particularly strong candidates for reliable UV detection especially where there is a need for single-photon counting capabilities.[1] However, numerous material-, fabrication-, technology-, and design-related issues remain before GaN APDs can be commercialized.

Recently, there have been several groups reporting the development and characterization of front-illuminated GaN and AlGaN APDs.[1–4] In these devices, front illumination yields multiplication dominated by electron-initiated ionization, since high-quality III-nitride growth typically requires that *p* layers are grown at the top of *p-n* and *p-i-n* structures. However, theory has predicted a significantly higher hole ionization coefficient,[5] and hence higher multiplication factors and lower excess noise are expected for back-illuminated GaN *p-i-n* diodes, contrary to most other III-V semiconductors. Back illumination also allows easier integration and packaging layouts through flip-chip technology as required for the production of APD arrays.[6] However, although a few works have assessed back illumination in AlGaN APDs,[7,8] none have done so in GaN APDs. The main issues for UV back-illuminated GaN APDs are the limitation of absorption in the GaN below the active region and the problem of the interface quality between the GaN device structure and the transparent template layer. In this work, we report on the growth, fabrication, and characterization of back-illuminated GaN APDs on thick AlN templates. Comparison of the performance of these same devices under front and back illumination allows us to reach a better understanding of carrier multiplication in this material and to determine experimentally both electron and hole ionization coefficients.

p-i-n samples were grown in an Aixtron 200/4-HT metal-organic chemical vapor deposition reactor on double-side polished sapphire substrates. The template consists of 500 nm of high-quality AlN grown by atomic layer epitaxy atop a 20 nm low-temperature AlN nucleation layer, similar to that discussed in our previous papers.[9] The *p*- and *n*-GaN layers consist of Mg- and Si-doped GaN, respectively, while the intrinsic region consists of unintentionally doped GaN. Twelve samples were grown. Layer thicknesses ranged from 100 to 640 nm for the *p*-type region and from 100 to 400 nm for the *n*-type region; the thickness of the intrinsic layer was varied from 0 to 200 nm.

Carrier concentrations in these layers were estimated by Hall-effect measurement of test samples, yielding values in the 10^{16} range for the electron concentration in the intrinsic layer, $(1-3)\times10^{18}$ cm^3 for the hole concentration in the *p*-GaN layer, and $(1-2)\times10^{18}$ cm^3 for the electron concentration in the *n*-GaN. Each device has an area of 25×25 μm^2 defined by squared mesas, which form a two-dimensional array of 320×256 detectors surrounded by a single common Ohmic Ti/Au (400 Å/1200 Å) *n*-type contact. A 15×15 μm^2 thin Ni/Au (30 Å/30 Å) *p*-type contact was evaporated on top of the mesas, annealed, and then followed by a thick Ti/Au (400 Å/1200 Å) top contact. Devices were passivated with 300 nm of SiO_2 and 10×10 μm^2 windows were opened.

Current-voltage (*I-V*) measurements were performed on the *p-i-n* diodes, and the breakdown characteristics were observed to vary as a function of the different layer thicknesses. Two illustrative *I-V* characteristics under reverse bias are shown in Fig. 1 for samples A (*p*-100 nm/*i*-200 nm/*n*-100 nm/AlN) and B (*p*-285 nm/*i*-150 nm/*n*-400 nm/AlN). Breakdown voltage (V_{bd}) reduced from 102 V for sample A to 78 V for sample B, as a consequence of the narrower intrinsic region. The inset of Fig. 1 shows V_{bd} as a function of *i*-region thickness for all the samples under study. From fitting the data with a simple abrupt junction model (assuming the potential is dropped across the intrinsic region), a critical electric field of 2.73 MV/cm is obtained; this is close to the previous values reported in the literature.[10,11] No significant variations of the breakdown voltages were observed with the thickness of the *p*-type or *n*-type layers. Sample C (*p*-285 nm/*i*-150 nm/*n*-400 nm/GaN:Si/GaN) was grown at the same time as sample B; however, instead of an AlN template, a GaN:Si/GaN (2 μm/1 μm) template was used. It makes the effective thickness of the *n*-GaN layer 2400 nm. Despite this modification, it is shown that the breakdown voltage remains the same.

[a)]Electronic mail: razeghi@ece.northwestern.edu

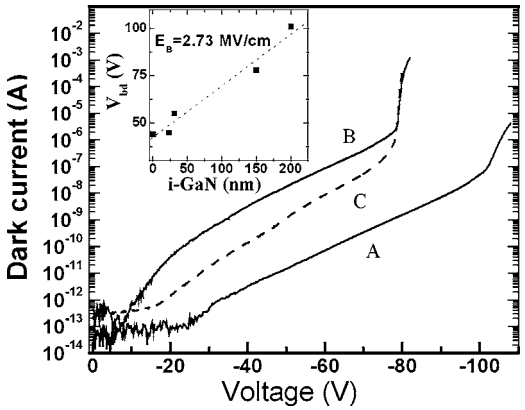

FIG. 1. Breakdown characteristics of samples A, B, and C are shown. Inset: The experimental breakdown voltages obtained for different thicknesses of the intrinsic layer.

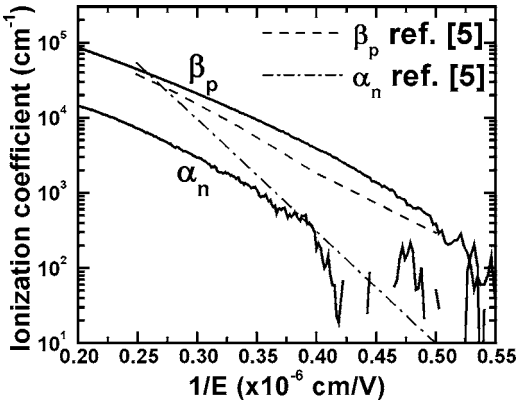

FIG. 3. Solid lines: Ionization factors obtained for electrons (α_n) and holes (β_p) from experiment. The dashed line and the dotted-dashed line represent theoretical values for β_p and α_n, respectively, as extracted from Ref. 5.

The series resistance of the diodes was calculated from the *I-V* characteristic under forward bias. Values between 465 and 3150 Ω were found for samples grown on AlN templates while the same structures grown on GaN:Si/GaN exhibited values between 29 and 190 Ω. The series resistance is dominated by the thickness of the *n*-GaN layer, increasing linearly with the inverse of it. This indicates that the conduction along the *n*-GaN/AlN interface is not a significant contribution for back-illuminated avalanche photodiodes.

The steepness of the avalanche characteristic is affected by the high series resistance created by thin *n*-GaN layers, and becomes softer. However, at the current levels obtained at the onset of breakdown, the effect of the series resistance is small, affecting the breakdown voltage by less than 1 V. This is shown in Fig. 1, in which the device with the thinnest *n*-GaN layer (sample A) presents a less abrupt breakdown characteristic. This effect is a handicap for the fabrication of devices operating in Geiger mode but at the same time helps keep moderate levels of dark current above breakdown and provides a higher stability for operation in linear mode. Dark current of sample A was monitored during more than 60 h of continuous operation 2 V above the breakdown voltage, finding a standard deviation of only 6%.

Photocurrent measurements of samples A and B were performed under back and front illumination with a 244 nm laser (optical power=102 W/cm^2). Shadowing effects of the metal contacts and probes cannot assure the same incident power for both illumination procedures; however, this is only a minor source of error for the gain of these devices. Both configurations allowed us to inject holes or electrons selectively into the active region to initiate the multiplication process. Multiplication factors were calculated from these measurements. Effects of the space-charge region spreading with voltage were taken into account by using a one-dimensional finite element model[12] of the device, which allowed us to fit the response at low voltages and to establish the photocurrent value corresponding to $M=1$. As observed in Fig. 2, back illumination provides higher gain than front illumination for both samples. The same result was obtained in all the *p-i-n* samples tested, regardless of the structure. Ionization events start at voltages above 50 V for holes and 70 V for electrons in sample A, and 35 and 65 V, respectively, in sample B. This agrees with the higher hole ionization coefficient that theory predicts, and which points to hole-initiated multiplication as a more beneficial concept in GaN.[5] The ionization coefficients for holes (β_p) and electrons (α_n) were calculated from the multiplication factors for electrons (M_n) and holes (M_p) as

$$\beta_p(E) = \frac{1}{W}\left(\frac{M_p(V)-1}{M_p(V)-M_n(V)}\right)\ln\left(\frac{M_p(V)}{M_n(V)}\right),$$

$$\alpha_n(E) = \frac{1}{W}\left(\frac{M_n(V)-1}{M_n(V)-M_p(V)}\right)\ln\left(\frac{M_n(V)}{M_p(V)}\right), \quad (1)$$

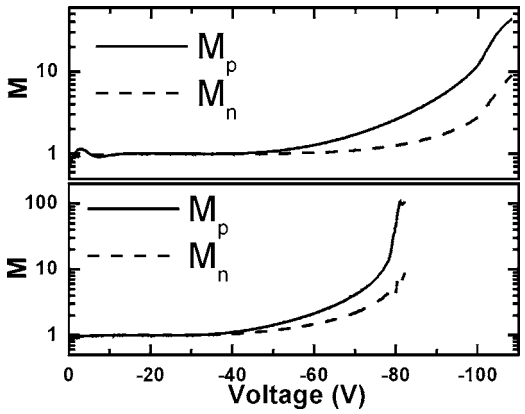

FIG. 2. Multiplication factors for electrons (M_n) and holes (M_p) obtained from sample A (top) and sample B (bottom).

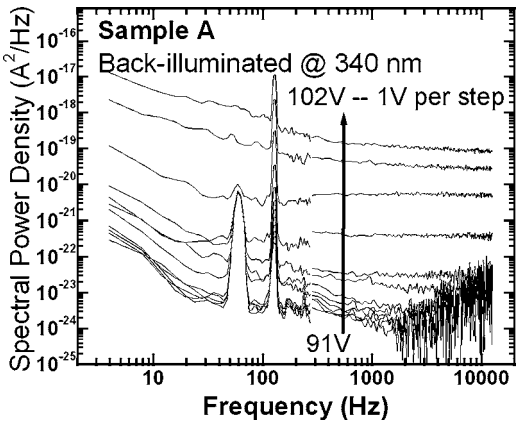

FIG. 4. Spectral power density (S_n) of sample A at the onset of breakdown is shown from 91 to 102 V with 1 V steps. The two narrow spikes at 60 and 120 Hz correspond to line noise.

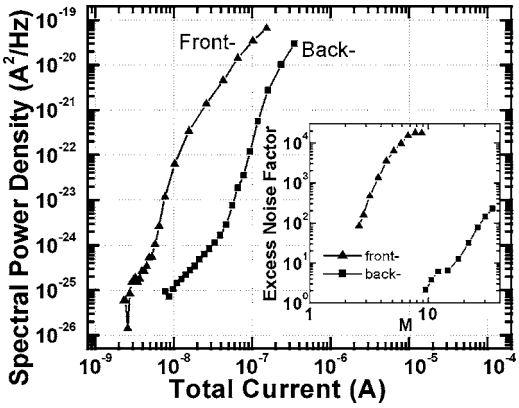

FIG. 5. Spectral power density is plotted as a function of total current for sample A under front (triangles) and back (squares) illumination. Inset: Calculated excess noise factors for front and back illumination.

and plotted in Fig. 3 assuming that the electric field (E) is constant across the i region (W) and equal to $E=V/W$.[13]

In addition, noise measurements were carried out on samples A and B under darkness and front and back illumination with a Xe lamp filtered at 340 nm (11 W/m^2). The signal from the detector was amplified with a low noise transimpedance amplifier with 1×10^7 V/A before analysis using a fast Fourier transform spectrum analyzer with a 100 kHz bandwidth. The noise floor of the system was in the 10^{-27} A^2/Hz range. Results for sample A under back illumination are shown in Fig. 4. It is noticeable that at low frequencies $1/f$ noise dominates. Spectral power density (S_n) for $1/f$ noise followed the relationship $S_n=s_0I^2/f^\gamma$, with average s_0 and γ values of 1.4×10^{-9} and $\leqslant0.33\pm0.05$, respectively, for sample A. In sample B, $\gamma=1.14\pm0.09$ and s_0 was at least three orders of magnitude higher, which suggests that the thin n-GaN plays a significant role in noise reduction. The γ value obtained for sample A is among the lowest values ever published in GaN. A strong reduction of $1/f$ noise has also been observed with thin n-GaN layers in previous works.[14]

At the onset of avalanche breakdown, a white noise contribution becomes dominant in the medium frequency range (1–30 kHz). To identify the origin of that noise, S_n was plotted against current for front and back illumination (Fig. 5). The rapid increase of the noise level with current suggests that it is likely to be excess multiplication noise. The excess noise factor (F) was calculated from $F=S_n/2qIM^2$, where q is the electron charge, I is the current under front or back illumination, and M is the multiplication factor (inset of Fig. 5). The results show that the excess multiplication noise factor is significantly lower under back illumination, confirming again the higher impact ionization coefficient for holes in GaN.

In summary, multiplication and noise characteristics of back-illuminated GaN APDs have been presented and compared with those provided by front illumination. This indicated that the hole initiated multiplication yields gain and noise characteristics with superior performances. The thickness of the n-GaN layer also plays a crucial role in the design of these devices.

The authors acknowledge the Fulbright Association and the Spanish Ministry of Education and Science for supporting one of the authors (J. L. P.), Motorola for supporting another author (K. M.), and the Richter Trust for supporting another author (R. M.). In addition, the authors would like to thank Donald Silversmith of the Air Force Office of Scientific Research for discussions and encouragement.

[1] K. A. McIntosh, R. J. Molnar, L. J. Mahoney, K. M. Molvar, N. Efremow, Jr., and S. Verghese, Appl. Phys. Lett. **76**, 3938 (2000).
[2] J. C. Carrano, D. J. H. Lambert, C. J. Eiting, C. J. Collins, T. Li, S. Wang, B. Yang, A. L. Beck, R. D. Dupuis, and J. C. Campbell, Appl. Phys. Lett. **76**, 924 (2000).
[3] A. Osinsky, M. S. Shur, R. Gaska, and Q. Chen, Electron. Lett. **34**, 691 (1998).
[4] T. Tut, S. Butun, B. Butun, M. Gokkavas, H. Yu, and E. Ozbay, Appl. Phys. Lett. **87**, 223502 (2005).
[5] I. J. Oguzman, E. Belotti, K. F. Brennan, J. Kolnik, R. Wang, and P. P. Ruden, J. Appl. Phys. **81**, 7827 (1997).
[6] DARPA BAA06-14, Deep Ultraviolet Avalanche Photodetectors (DUVAP), 2005.
[7] R. McClintock, A. Yasan, K. Minder, P. Kung, and M. Razeghi, Appl. Phys. Lett. **87**, 241123 (2005).
[8] T. Tut, M. Gokkavas, B. Butun, S. Butun, E. Ulker, and E. Ozbay, Appl. Phys. Lett. **89**, 183524 (2006).
[9] R. McClintock, A. Yasan, K. Mayes, D. Shiell, S. R. Darvish, P. Kung, and M. Razeghi, Proc. SPIE **5359**, 434 (2004).
[10] A. Nishikawa, K. Kamakura, T. Akasaka, and T. Makimoto, Appl. Phys. Lett. **88**, 173508 (2006).
[11] X. A. Cao, H. Lu, S. F. LeBoeuf, C. Cowen, S. D. Arthur, and W. Wang, Appl. Phys. Lett. **87**, 053503 (2005).
[12] D. Winston and R. Hayes, Inst. Phys. Conf. Ser. **141**, 747 (1995).
[13] G. Stillman and C. Wolfe, in *Semiconductors and Semimetals*, edited by R. Willardson (Academic, New York, 1977), Vol. 12, Chap. 5, p. 333.
[14] S. L. Rumyantsev, N. Pala, M. S. Shur, R. Gaska, M. E. Levinshtein, M. Asif Khan, G. Simin, X. Hu, and J. Yang, Electron. Lett. **37**, 720 (2001).